2 September 2002

ELSEVIER

Chemical Physics Letters 363 (2002) 34–38

CHEMICAL PHYSICS LETTERS

www.elsevier.com/locate/cplett

A facile vapor–solid synthetic route to Sb_2O_3 fibrils and tubules

Changhui Ye [1], Guowen Meng, Lide Zhang [*], Guozhong Wang, Yinhai Wang

Laboratory of Functional Nanomaterials and Nanostructures, Institute of Solid State Physics, Chinese Academy of Sciences, P.O. Box 1129, Hefei, Anhui 230031, China

Received 5 February 2002; in final form 4 June 2002

Abstract

Sb_2O_3 fibrils and tubules with lengths of up to several millimeters and diameters of nanometers to submicrometers were achieved by using Sb_2S_3 nanopowders as starting material. The synthesis can be ascribed to a vapor–solid process where metal catalyst was neither adopted during the synthesis, nor observed at tips of fibrils or tubules. Sb_2O_3 fibrils and tubules with lateral dimensions in nano- or submicron-scale may show enhanced catalytic and flame retardant performances. © 2002 Elsevier Science B.V. All rights reserved.

1. Introduction

The discovery of carbon nanotubes and semiconductor nanowires has initiated an exploding research field in which enormous efforts have been invested due to their fundamental significance to the study of size- and dimensionality-dependent chemical and physical properties [1–3]. During the past decade, a wide variety of nanowires have been successfully synthesized, including semiconductors (Si [4], GaN [5], ZnO [6], InP [7], etc.), metals (Au [8], Ag [9], Bi [10], etc.), superconductors (Pb [11], MgB_2 [12], etc.), and insulators (B [13], etc.). There are many synthetic mechanisms to produce nanowires, among which vapor–liquid–solid (VLS) mechanism is the most extensively explored case where metal particles are employed as catalysts and generally an alloy droplet presents on the growth tip of each nanowire [14]. Solution–liquid–solid (SLS) mechanism [15], vapor–solid (VS) mechanism [16,17], and oxide-assisted growth mechanism [18] have also been adopted to synthesize various nanowires. Recently, Sb_2O_3 nanorods have been synthesized by using microemulsion [19] and templating carbon nanotubes [20] by several groups, however, very long Sb_2O_3 fibers and tubes have never been reported. In this Letter, we demonstrate an alternative approach to the synthesis of Sb_2O_3 fibrils and tubules with diameters of several tens to hundreds of nanometers and lengths of up to several millimeters by the VS method.

2. Experimental

Sb_2S_3 powders (ca. 50 nm), obtained via a direct reaction of $Sb(NO_3)_3$ and Na_2S in aqueous solution, were used as starting material. The self-pre-

[*] Corresponding author. Fax: +86-551-5591434.
E-mail address: ldzhang@mail.issp.ac.cn (L. Zhang).
[1] Also corresponding author.

0009-2614/02/$ - see front matter
PII: S0009-2614(02)01018-7

pared Sb_2S_3 powders were loaded in a ceramic boat and placed in the middle of a ceramic tube in a horizontal furnace, and a silicon wafer was located downstream in the ceramic tube. The furnace was heated to 773 K in 3 min and held at this temperature for 90 min. High-purity argon was used as carrier medium at a constant flow rate of 80 sccm during the heating process. After cooling down of the furnace, lots of light yellow fluffy materials were observed on the silicon wafer, which were examined with scanning electron microscopy (SEM), transmission electron microscopy (TEM), energy dispersive X-ray spectroscopy (EDX), X-ray diffraction (XRD), and X-ray photoelectron spectroscopy (XPS).

3. Results and discussion

The morphology of the as-synthesized product is shown in the SEM image (Fig. 1a). The Sb_2O_3 fibrils and tubules are fairly straight with diameters typically in the range of 50–350 nm and lengths of up to several millimeters. Particles and platelets are observed occasionally while fibrils and tubules are the dominant products. Two tubules with outer diameters of 140 nm (upper left) and 60 nm (lower right) are indicated in Fig. 1b with the tube openings marked by arrowheads, respectively. Tubes with broken tips (Fig. 1b) and platelets with partially closed tubular structures (Fig. 1c) are also observed, suggesting the formation of tubules from bending of platelets as will be discussed later. Several fibrils are also displayed in the same image. To further examine the crystalline structure and crystallography of the products, TEM was performed. In Fig. 2a, a Sb_2O_3 tube with outer diameter of 120 nm and wall thickness of 50 nm is shown. One 80-nm-diameter Sb_2O_3 fibril is shown in Fig. 2b, and it is noticed that this fibril is smooth and straight. The selected area electron diffraction (SAED) pattern (inset) further demonstrates the single crystallinity of this nanofibril. As should be note here, although Sb_2O_3 has a melting point higher than 700 K, it seems not very stable under the illustrating of high-energy beams in TEM, henceforth high-resolution image of the Sb_2O_3 fibrils and tubules could not be obtained.

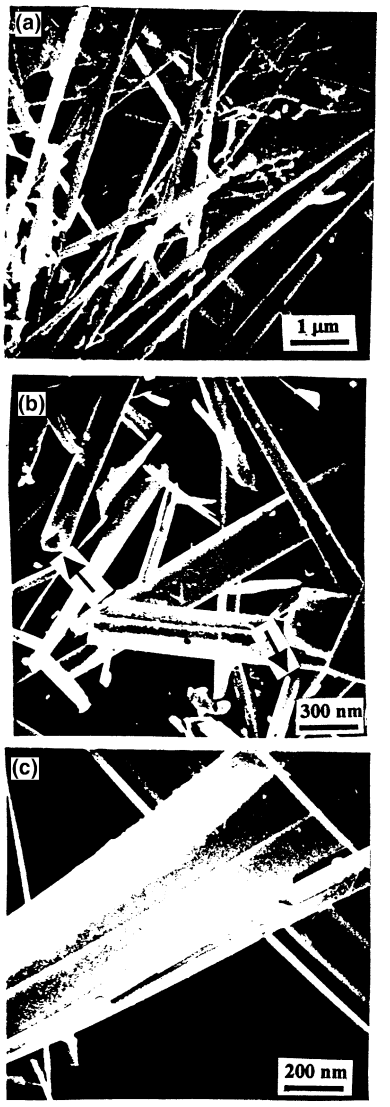

Fig. 1. SEM images of Sb_2O_3 tubules. (a) Morphology at low-magnification. (b) High-magnification image of Sb_2O_3 fibril and tubular structures, with arrowheads marking the openings and the broken tips of the tubules. (c) Broken-bamboo-shaped tubule.

In addition, XRD is also performed to examine the crystalline structure and phase purity of the Sb_2O_3 fibrils and tubules. In Fig. 3, all the peaks in the XRD pattern can be readily indexed to the cubic phase of Sb_2O_3 with lattice constant of 1.14 nm that is consistent with the standard value (JCPDS 5-0543, $a = 1.152$ nm). It is surprisingly

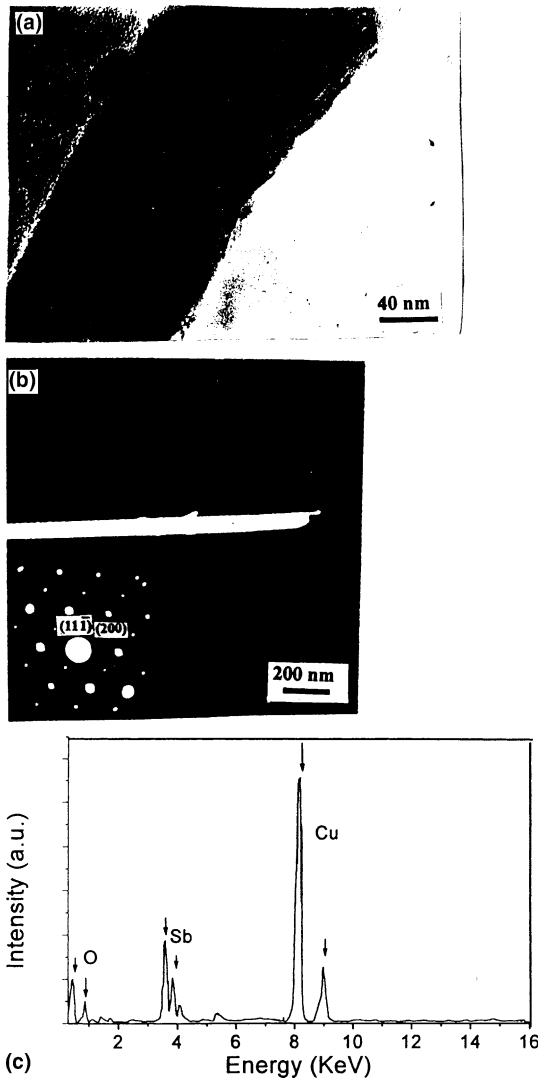

Fig. 2. TEM images. (a) One 120-nm-diameter Sb_2O_3 tubule with wall thickness ~50 nm. (b) One 60-nm-diameter Sb_2O_3 fibril. (Inset, SAED pattern of this Sb_2O_3 fibril taken along [0 1 1] zone axis clearly demonstrates the single crystallinity of the product.) (c) EDX spectrum shows only O, Sb, and Cu, without evidence of S being detected.

noticed that no phases of Sb_xS_y are present in the final product. To further prove this, XPS and EDX were carried out to investigate the composition and valence state of the element in the product. Fig. 4a is an overall element analysis and no sulfur element is detected in several batches of the similarly prepared products. It can be found

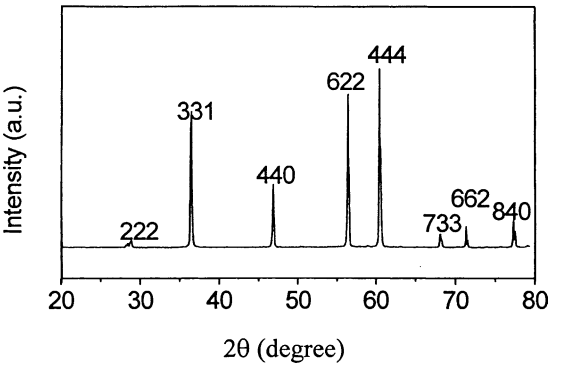

Fig. 3. XRD pattern of the product. All the peaks can be readily indexed to a cubic Sb_2O_3 phase.

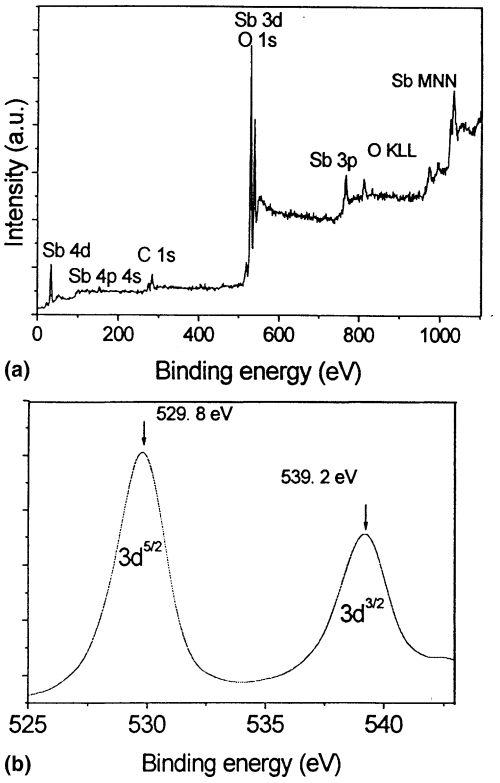

Fig. 4. (a) XPS spectrum of the product shows only O, Sb, and C, without S being detected. (b) The two Sb 3d peaks further prove that Sb is in Sb^{3+} state rather than Sb^{5+} state.

out that O and Sb elements are present at an atomic ratio of 1.72–1, which agrees well with the EDX data (Fig. 2c) within experimental error. The valence state of Sb in the product is confirmed as

Sb^{3+} rather than Sb^{5+} based on the fact that the binding energies obtained from Fig. 4b (Sb $3d^{5/2}$ 529.8 eV and Sb $3d^{3/2}$ 539.2 eV) are characteristic values of Sb^{3+} instead of Sb^{5+} which peaks at higher energies [21].

Since neither metal particles are present at the tips of either fibrils or tubules (see Figs. 1 and 2), nor metal catalyst was adopted in this synthesis, the well-known VLS growth mechanism could be ruled out as the appropriate mechanism in this synthesis. Instead, on the basis of the present results and the literatures [16,17], VS mechanism might be responsible for the growth of the Sb_2O_3 fibrils and tubules. The growth may involve three steps proposed as follows.

Firstly, in the high temperature zone, Sb_2S_3 evaporates and decomposes [22],

$$Sb_2S_{3(g)} \rightarrow 2SbS_{(g)} + 1/2S_{2(g)} \quad (1)$$

$$SbS_{(g)} \rightarrow Sb + S_{(g)} \quad (1')$$

Secondly, SbO and Sb vapor are transported to a lower temperature zone by Ar and solidifies locally on the silicon wafer to form nuclei.

Thirdly, with the presence of O_2 in the furnace (O_2 could come from the leakage of the furnace, considering that the Si wafer was thoroughly treated with HF solution prior to use and the high-purity of Ar we employed), SbS (Sb as well) molecules are oxidized to give Sb_2O_3 [23],

$$\begin{aligned} SbS_{(g)} + O_{2(g)} &\rightarrow Sb_2O_{3(s)} + SO_{2(g)} \\ Sb_{(g)} + O_{2(g)} &\rightarrow Sb_2O_{3(s)} \end{aligned} \quad (2)$$

the Sb_2O_3 molecules grow on the nuclei as fibrils or platelets. The fibrils are believed to form according to helical dislocation growth model of VS mechanism, which is evidenced by the round tapering tip of the Sb_2O_3 fibril shown in Fig. 2b. However, the growth of tubules may involve bending of the platelets, which has already been well documented to account for the growth of various nanotubes such as carbon [1], WS_2 [25], and MoS_2 [26]. Considering the inherent chain type as well as pseudo-two-dimensional structure of Sb_2O_3 [23], and recalling the partially closed, broken bamboo like structure in Figs. 1b and c, the formation of Sb_2O_3 fibrils and tubules via VS mechanism under appropriate experimental conditions is both plausible and feasible.

4. Conclusion

In summary, we have synthesized Sb_2O_3 fibrils and tubules via a VS growth mechanism. It is well known that Sb_2O_3 can be used as an effective catalyst in photochemistry individually or combined with other oxides and is also widely employed as efficient flame retardant [21,24]. With the reduction of the lateral scale, especially with a hollow inner structure, this kind of materials may demonstrate much better catalytic performance. Further study on the growth mechanism at atomic scale and catalytic properties is under way.

Acknowledgements

This work was supported by the National Natural Science Foundation of China (Grant No. 10074064 and 19974055) and 973 key project. We thank Prof. Weiping Cai, Prof. Guanghai Li, and Dr. Zhi Jiang for valuable discussions.

References

[1] S. Iijima, Nature 354 (1991) 56.
[2] J. Hu, T.W. Odom, C.M. Lieber, Acc. Chem. Res. 32 (1999) 435.
[3] S.M. Prokes, K. Wang, Mater. Res. Soc. Bull. 24 (1999) 13.
[4] Y. Zhang, Y. Tang, N. Wang, D. Yu, C.S. Lee, L. Bello, S.T. Lee, Appl. Phys. Lett. 72 (1998) 1835.
[5] W. Han, S. Fan, Q. Li, Y. Hu, Science 277 (1997) 1287.
[6] M.H. Huang, Y. Wu, H. Feick, N. Tran, E. Weber, P. Yang, Adv. Mater. 13 (2001) 113.
[7] X. Duan, Y. Huang, Y. Cui, J. Wang, C.M. Lieber, Nature 409 (2001) 66.
[8] Y. Kondo, K. Takayanagi, Science 289 (1999) 606.
[9] S. Bhattacharrya, S.K. Saha, D. Chakaravorty, Appl. Phys. Lett. 76 (2000) 3896.
[10] Y.M. Lin, S.B. Cronin, J.Y. Ying, M.S. Dresselhaus, J.P. Heremans, Appl. Phys. Lett. 76 (2000) 3944.
[11] G. Li, W. Schwarzacher, Appl. Phys. Lett. 74 (1999) 1746.
[12] Y. Wu, B. Messer, P. Yang, Adv. Mater. 13 (2001) 1487.
[13] L. Cao, Z. Zhang, L. Sun, C. Gao, M. He, Y. Wang, Y. Li, X. Zhang, G. Li, J. Zhang, W. Wang, Adv. Mater. 13 (2001) 1487.

[14] R.S. Wagner, W.C. Ellis, Appl. Phys. Lett. 4 (1964) 89.
[15] J.D. Holmes, K.P. Johnston, R.C. Doty, B.A. Korgel, Science 287 (2000) 1471.
[16] Z. Pan, Z. Dai, Z.L. Wang, Science 291 (2001) 1947.
[17] P. Yang, C.M. Lieber, J. Mater. Res. 12 (1997) 2981.
[18] N. Wang, Y. Tang, Y. Zhang, C.S. Lee, S.T. Lee, Phys. Rev. B 58 (1998) R16024.
[19] L. Gui, Z. Wu, T. Liu, W. Wang, H. Zhu, Chem. Phys. Lett. 318 (2000) 49.
[20] S. Friedrichs, R.R. Meyer, J. Sloan, A.I. Kirkland, J.L. Hutchison, M.L.H. Green, Chem. Commun. 929 (2001).
[21] U.-A. Schubert, F. Anderle, J. Spengler, J. Zuehlker, H.-J. Eberle, R.K. Grasselli, H. Knoezinger, Top. Catal. 15 (2001) 195.
[22] A.S. Pashinkin, Zh. Fiz. Khim. 38 (1964) 2690.
[23] S. Xiang, X. Yang, T. Cao, in: Inorganic Chemistry Series, vol. 4, Scientific Press, 2000, p. 482.
[24] B. Pillep, P. Behrens, U.-A. Schuber, J. Spengler, H. Knoezinger, J. Phys. Chem. B 103 (1999) 9595.
[25] R. Tenne, L. Margulis, M. Genut, G. Hodes, Nature 360 (1992) 444.
[26] M. Remskar, Z. Skraba, Appl. Phys. Lett. 69 (1996) 351.